Clays and Clay Minerals, Vol. 56, No. 4, 470–485, 2008.

LOW-TEMPERATURE FTIR STUDY OF KAOLIN-GROUP MINERALS

CLIFF T. JOHNSTON[1,*], JESSICA ELZEA KOGEL[2], DAVID L. BISH[3], TOSHIHIRO KOGURE[4], AND HAYDN H. MURRAY[3]

[1] Crop, Soil and Environmental Sciences, Purdue University, 915 W. State Street, West Lafayette, IN 47907-2054, USA
[2] IMERYS, Sandersville, GA 31082, USA
[3] Department of Geological Sciences, Indiana University, Bloomington, IN 47405, USA
[4] Department of Earth and Planetary Science, Graduate School of Science, The University of Tokyo, 7-3-1 Hongo, Bunkyo-ku, Tokyo, 113-0033 Japan

Abstract—Low-temperature FTIR spectroscopy was used to characterize the ν(OH) region of kaolin-group minerals including well ordered to poorly ordered kaolins from Georgia, Brazil, and England, along with samples of discrete dickite and nacrite. Low-temperature FTIR spectra were useful in resolving dickite- and nacrite-like features present in the spectra of kaolins when cooled to <30 K. These features were not resolved at room temperature and only partially resolved at liquid N_2 temperature (77 K). The room-temperature and low-temperature positions of the ν(OH) bands of kaolinite, dickite, and nacrite were linearly correlated with the interatomic OH···O distances and this relationship served as the basis for polytype/disorder identification. Dickite or dickite-like disorder was found in high Hinckley-Index kaolinite from Keokuk, Iowa, and from Cornwall, England. Dickite- and nacrite-like features were observed in both high- and low-Hinckley-index kaolinite and the amounts of these stacking sequences generally increased with decreasing Hinckley Index.

Key Words—Dickite, FTIR Spectroscopy, Hinckley Index, Kaolin-group Minerals, Kaolinite, Low-temperature FTIR Spectroscopy, Nacrite, Structural Disorder.

INTRODUCTION

Kaolin-group minerals (KGMs) are among the most abundant and industrially important clay minerals on Earth. Consequently, the nature and extent of disorder in these minerals has been the subject of sustained interest during the past half century (Murray, 1954; Brindley *et al.*, 1986; Giese, 1990; Fialips *et al.*, 2001; Reynolds and Bish, 2002). A useful starting point to understand structural disorder in KGMs is to consider the structural differences between the polytypes. Although there are many possible ways of stacking the individual dioctahedral 1:1 layers in KGMs (Dornberger-Schiff and Ďurovič, 1975), only three polytypes have been found in nature to date. Kaolinite is the most abundant form, dickite is considerably less common, and occurrences of nacrite are rare. These polytypes share the same fundamental unit layer ($Al_2Si_2O_5(OH)_4$) which comprises one Si-tetrahedral sheet sharing apical oxygen atoms with an Al-octahedral sheet.

The structural OH groups that terminate the Al-octahedral sheet form long hydrogen bonds with the opposing siloxane surface of the neighboring tetrahedral sheet (Hendricks, 1938; Bailey, 1963; Bailey, 1988). Hendricks (1938) was among the first to show that the various polytypes of KGMs are determined to a large extent by these interlayer $OH\cdots O_{siloxane}$ pairings, and that each polytype is characterized by a unique set of long interlayer hydrogen bonds with interlayer OH···O distances ranging from 0.29 to 0.315 nm. The structures of the fundamental 1:1 layer ($Al_2Si_2O_5(OH)_4$) and of kaolinite, dickite, and nacrite projected along the [100] and [010] axes are shown in Figure 1. In addition, the $OH\cdots O_{siloxane}$ distances of the three interlayer hydrogen bonds are given to the right of each. A detailed structural comparison of the three polytypes is beyond the scope of this paper other than to point out that each polytype is characterized by a unique set of long interlayer hydrogen bonds. Although other factors contribute to the interlayer stacking energetics of KGMs, including the positions of the hydrogen atom, non-linearity of the OH···O bonds, and registration of the vacant octahedral sites between layers, the largest determinant is minimization of the combined lengths of these long interlayer hydrogen bonds (Bailey, 1963; Giese and Datta, 1973; Giese, 1973; Bailey, 1988).

From an energetic point of view, high-temperature oxide-melt solution calorimetry of kaolinite, dickite, and nacrite showed that the standard Gibbs free energy of formation of dickite and nacrite was less negative than kaolinite by values ranging from 12 to 25 kJ/mol, indicating that kaolinite is thermodynamically stable relative to dickite and nacrite (de Ligny and Navrotsky, 1999; Fialips *et al.*, 2001; Fialips *et al.*, 2003). However, formation energies derived from first-principle

* E-mail address of corresponding author:
clays@purdue.edu
DOI: 10.1346/CCMN.2008.0560408

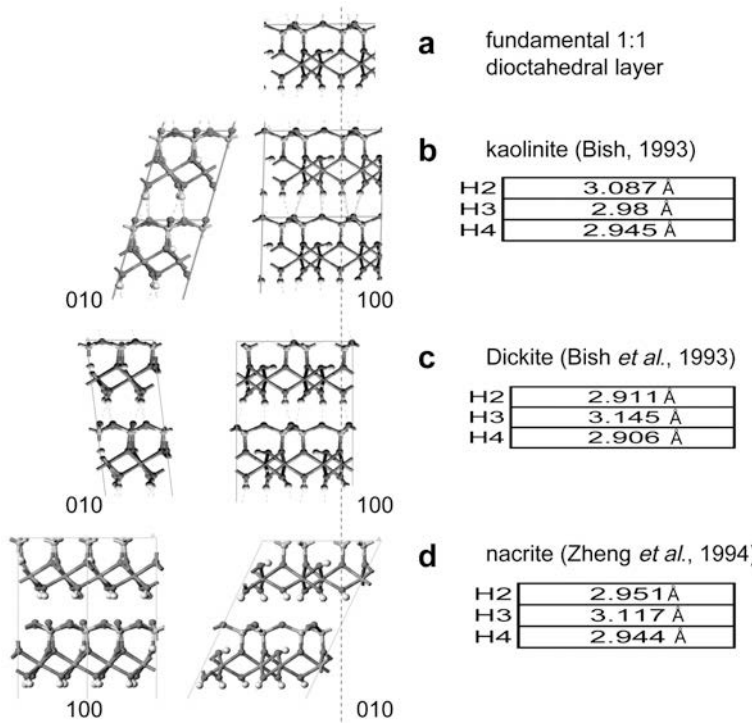

Figure 1. Projection of (a) fundamental 1:1 dioctahedral layer; (b) kaolinite; (c) dickite; and (d) nacrite along [100] and [010]. In the case of nacrite, the crystallographic axes are reversed such that the [100] projection compares with the [010] projections for kaolinite and dickite. The interlayer OH···O distances (Å) for the three polytypes are listed on the right of the figure.

calculations using density functional theory were very similar (Benco *et al.*, 2001b; Sato *et al.*, 2004; Balan *et al.*, 2005). In addition, experimental solubility measurements indicate that the difference in Gibbs free energy between kaolinite and dickite is smaller than that obtained from high-temperature calorimetric measurements (Zotov *et al.*, 1998). Although the occurrence of dickite was first associated with hydrothermal activity, it is now commonly identified with authigenic kaolins in sandstone reservoirs (Ehrenberg *et al.*, 1993; Lanson *et al.*, 1996; Beaufort *et al.*, 1998). In contrast to the thermochemical data, Lanson *et al*. (2002) argued on the basis of burial diagenesis that dickite is the stable polytype. Kaolinite was the dominant polytype found in shallow buried sandstones at depths <2000 m. However, the transformation of kaolinite to dickite occurred over the depth range 2500–5000 m, and dickite was the dominant polytype below 5000 m.

Many methods have been used to study structural disorder in KGMs including, but not limited to, X-ray diffraction (XRD), infrared (IR) and Raman spectroscopy, high-resolution transmission electron microscopy (HRTEM), nuclear magnetic resonance (NMR), electron spin resonance (ESR), thermal analysis, and computational methods. Until recently, the only quantitative models of structural disorder in KGMs were based on analysis of X-ray powder diffraction data. Hinckley (1963) described a simple, qualitative 'crystallinity index' based on the ratio of the sum of the heights of the 110 and 111 reflections to the height of the 110 reflection from kaolinite. This index, although widely cited, is not based on an accurate model of kaolinite disorder and is therefore of limited use for interpreting the nature of structural disorder in a particular sample.

Structural disorder in KGMs causes the XRD reflections to degrade in different ways, depending on the nature of the defect. Over the past 25 y, a number of quantitative models have been proposed to describe structural disorder in kaolinite (Plançon and Tchoubar, 1977; Barrios *et al.*, 1977; Plançon *et al*., 1989; Bookin *et al.*, 1989; Plançon and Zacharie, 1990; Plançon, 2001). These models assume different types of disorder, all embodied in a mathematical model providing a simulated diffraction pattern. The accuracy of the models has been assessed by evaluating how well the simulated patterns reproduce measured diffraction patterns. Thus the types and degree of disorder are not determined directly from measured diffraction patterns. At present, structural disorder in KGMs is attributed primarily to three types of defects that include (1) defects in the position of the vacant octahedral site (B *vs*. C); (2) defects resulting from interlayer translation directions; and (3) modification of these interlayer translations by random shifts (Reynolds and Bish, 2002). In general, overall consensus on the specific types of structural defects present has not been reached because

https://doi.org/10.1346/CCMN.2008.0560408 Published online by Cambridge University Press

the structural defects cannot be probed directly but are inferred on the basis of degraded XRD patterns.

Recently, Kogure and Inoue (2005a, 2005b) examined structural disorder in kaolinite and dickite using HRTEM with sufficient resolution to distinguish defect structures directly in certain kaolins. They obtained images of kaolinite and dickite along X_i <(i = 1 to 3, see Bailey (1988))> directions, to distinguish the vacant octahedral site position and interlayer transition for individual layers. Selected area electron diffraction (SAED) images recorded parallel to [100] of a dickite of diagenetic origin showed no streaking and HRTEM images indicated regular alternation between B and C sites; no stacking faults were found (Kogure and Inoue, 2005a, 2005b). In contrast, HTREM images of a disordered kaolinite in the same origin showed significant disorder due to the two alternative ($-a/3$ and $-a/3 + b/3$) interlayer translations, but no defect structures resulting from defects in the position of the vacant octahedral site (*i.e.* presence of dickite-like stacking sequences in the kaolinite crystal) were observed (Kogure and Inoue, 2005a). In a related study of a kaolin specimen collected from a hydrothermal deposit, HRTEM images showed a more complex distribution of disordered sites, including alternation of the vacant octahedral sites and disorder from interlayer transitions (Kogure and Inoue, 2005b). An exciting part of Kogure's recent work is that structural defects in kaolinite were observed directly, for the first time, using HRTEM. Unfortunately, KGMs deteriorate rapidly in the intense electron beam that is required to record HRTEM images and generally only KGMs with large crystals (~several μm) are amenable to analysis by HRTEM.

As emphasized above, the details of interlayer OH···O interactions are very important in determining the nature of layer stacking in KGMs. X-ray diffraction is intrinsically insensitive to variations in H atom position because of the small X-ray scattering factor of the H atom (Moore and Reynolds, 1989; Post and Bish, 1989). This has led a number of researchers to IR and Raman spectroscopy which provide complementary information about the structural OH groups (Ledoux and White, 1964; Johnston *et al.*, 1985; Michaelian, 1986; Prost *et al.*, 1989; Johnston *et al.*, 1990; Johnston *et al.*, 1998; Farmer, 1998; Shoval *et al.*, 2001). In particular, the well resolved stretching vibrations of the structural OH groups of KGMs have long been recognized as sensitive 'reporter groups' to subtle changes in their local environment. Low-temperature IR methods were first used by Prost and co-workers to study KGMs (Prost, 1984a, 1984b; Prost *et al.*, 1987, 1989). They showed that the low-temperature IR spectra of kaolinite, dickite, and nacrite were distinct and that the IR spectra of disordered kaolinite exhibited both dickite- and nacrite-like features. In addition Brindley *et al.* (1986) used low-temperature FTIR spectroscopy, along with powder XRD, chemical analysis, particle-size distribution measurements, and electron spin resonance (ESR), to study structural disorder in a diverse group of KGMs. Their low-temperature FTIR spectra showed significant spectral variation among the different kaolin samples analyzed but definitive conclusions based on the FTIR spectra were not possible. This was due, in part, to the fact that their spectra were obtained at liquid nitrogen temperatures, which was insufficient to clearly resolve the ν(OH) features of KGMs. In a low-temperature FTIR study of dickite, we showed that cooling to temperatures of <30 K is necessary to fully resolve the ν(OH) bands (Bish and Johnston, 1993). The primary objective of the present study was to examine a diverse group of kaolin specimens using low-temperature FTIR spectroscopy. Our goal was to evaluate whether low-temperature spectroscopic methods can provide new insight into disorder in KGMs.

SAMPLES

Ten kaolin samples representing both primary and secondary occurrences, a dickite sample, and a nacrite sample were analyzed in this study (Table 1). The samples were selected to include both poorly ordered, low-Hinckley index (HI) kaolins and well ordered, high-HI kaolinite. The bulk of the samples were secondary kaolins from the US (Georgia and New Mexico) and Brazil. Two of the Georgia kaolins (I-B and IV-L) were described previously by Brindley *et al.* (1986) and were generously given to the authors by J.L. Harrison. Three Brazilian kaolins were analyzed, consisting of two soft, well ordered kaolins from the Amazon basin, referred to as the Capim and Patinga kaolins, and the Jari kaolin, a poorly ordered hard kaolin. The Capim and Patinga kaolins are mined ~180 km south of Belém from the Tertiary Ipixuna Formation. The primary kaolins examined are from Cornwall, England, and Keokuk, Iowa. The Cornwall kaolin formed from hydrothermal alteration of granite (Dominy and Camm, 1998) and the very pure, well ordered Keokuk kaolinite occurs as large kaolinite crystals found in geodes (Keller and Haenni, 1978).

Dickite from Saint Claire, Pennsylvania, and nacrite from the Lodéve Basin, France, (sample obtained from M. Buatier) were also included in the study. The Saint Claire dickite was selected for this study because it is a well known example of high-purity, low-defect dickite that has been thoroughly studied using a variety of techniques including FTIR (Johnston *et al.*, 1990), X-ray and neutron powder diffraction (*e.g.* Bish and Johnston, 1993), Raman spectroscopy (Johnston *et al.*, 1998), and calorimetry (De Ligny and Navrotsky, 1999; Fialips *et al.*, 2003). Similarly, the nacrite specimen was described by Buatier *et al.* (2000) and it occurs in dolomite cavities in Cambrian basement of the Permian basin and is associated with barite of hydrothermal origin.

https://doi.org/10.1346/CCMN.2008.0560408 Published online by Cambridge University Press

Table 1. Description of samples studied, location of the sample. The designation P or S is the approximate designation as primary or secondary origin, respectively. The Hinckley Index and source of the kaolin are listed.

Dominant polytype	Sample	Location	Type	HI	% ldp	Source
Kaolinite	Keokuk	Iowa, USA	P	1.50		W.D. Keller Memorial Collection
	Cornwall	Cornwall, England	P	1.07	33.9	Haydn Murray
	Mesa Alta	New Mexico, USA	S			API Standard No. 9
	Wilkinson County I-B	Georgia, USA	S	1.52		Brindley
	Warren County IV-L	Georgia, USA	S	0.32		Brindley
	Washington County	Georgia, USA	S	1.02	21.9	Thiele Kaolin Co.
	McDuffie County	Georgia, USA	S	0.46	0	Thiele Kaolin Co.
	Patinga	Brazil	S	1.30		Haydn Murray
	Rio Jari	Brazil	S	0.37	0	Haydn Murray
	Capim	Brazil	S	1.12	36.2	Haydn Murray
Dickite	Dickite	St. Claire, Pennsylvania	P			Charles Roth
Nacrite	Nacrite	France	P			Martine Buatier

P = primary origin
S = secondary origin

METHODS

Low-temperature FTIR spectroscopy

Low-temperature FTIR spectra were obtained using a Perkin Elmer 2000/GX spectrometer equipped with a liquid-N_2-cooled MCT detector. The unapodized spectral resolution was 1.0 cm^{-1}. A total of 256 scans were co-added for each spectrum. The FTIR spectra were obtained in transmission using a Nujol mull (Johnston and Aochi, 1996) by mixing 2 mg of clay with a few drops of mineral oil and placing the mull between two CaF_2 windows. The kaolin samples were analyzed as received. The windows were mounted on the cold finger of an Air Products D200 Displex using an indium gasket. To avoid condensation on the windows, the sample chamber in the Displex was evacuated to a pressure of 10^{-6} mm Hg. Temperature was measured using a Au:Chromel thermocouple. Additional details about the low-temperature FTIR methods were reported elsewhere (Bish and Johnston, 1993; Wang and Johnston, 2000). Spectra were analyzed with Grams 32/AI (Versions 6.00) (Thermo Scientific Industries, Waltham, Massachusetts). Band positions and band widths were determined using the Peak-Fitting module of the *Grams* software. Spectra were fitted using a non-linear, least-squares fitting routine within Grams 32/AI and individual bands were represented by bands with mixed Gaussian-Lorentzian lineshapes and a simple two-point baseline correction.

X-ray diffraction

Analysis by XRD was performed on both oriented and random powder mounts with a Scintag PAD V diffractometer using CuKα radiation and a solid-state detector. The XRD patterns from random powder mounts were used to calculate the HI for each sample. Sample preparation for these analyses consisted of pulverizing 100 g of dry kaolin in a laboratory pulverizer. A recently published study has demonstrated that severe grinding is required to produce disordered material (Reynolds and Bish, 2002), thus increasing the amount of disordered kaolinite relative to the unground sample. The grinding conditions used in our laboratory did not cause an increase in kaolinite disorder as measured by HI. Structural parameters for dickite were obtained from Bish and Johnston (1993) and from Joswig and Drits (1986).

Particle-size fractionation and analysis

Naturally occurring kaolins are often made up of mixtures of well ordered and poorly ordered kaolinite crystals having a range of particle sizes and shapes (Keller, 1977; Plançon *et al.*, 1989; White *et al.*, 1998; Bish and Chipera, 1998; Bish and Chipera, 1999). Because we were interested in elucidating the mineralogy of individual particle size fractions, one sample (Capim from the Rio Capim mining district in Brazil) was dispersed with sodium hexametaphosphate and centrifuged to isolate the 2−0.5 μm, 0.5−0.2 μm, and the <0.2 μm fractions.

This sample was analyzed using an Horiba LA-910 laser diffraction particle size analyzer. Sample preparation consisted of dispersing 14 g of dry clay with a 0.1% solution of sodium hexametaphosphate to make a 7% solids slurry suspension. The suspension was mixed for 5 min using a Waring Blender.

SELECTED AREA ELECTRON DIFFRACTION (SAED)

The SAED patterns were obtained only from the Capim sample in order to investigate stacking disorder. The TEM specimens were prepared using Ar ion milling

https://doi.org/10.1346/CCMN.2008.0560408 Published online by Cambridge University Press

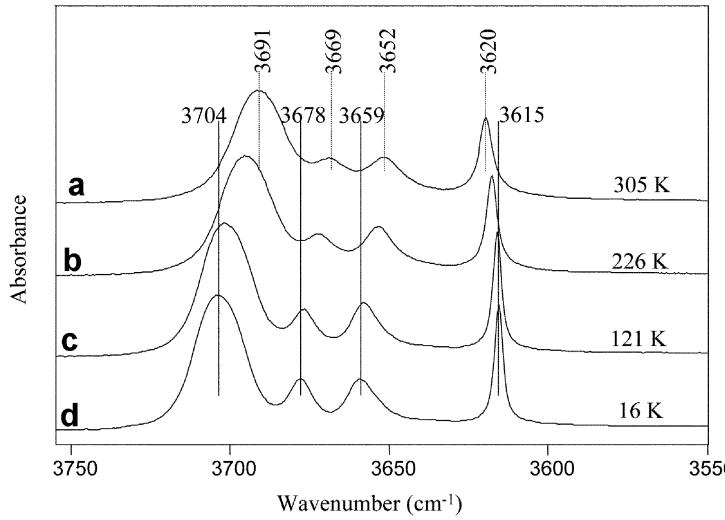

Figure 2. FTIR spectra of the Wilkinson County I-B sample (Georgia, USA) collected at temperatures ranging from room temperature to 16 K.

as described in previous work (Kogure and Inoue, 2005a). A JEOL JEM-2010 TEM device with a high-resolution pole piece (Cs = 0.5 mm) was used at 200 kV. The pattern was recorded with an SA aperture the diameter of which corresponds to ~100 nm and with a CCD camera (Gatan MSC 794).

RESULTS

Influence of temperature on the ν(OH) bands of kaolinite

Of the Georgia kaolins studied, the Wilkinson County I-B sample had the largest HI (Table 1) with a value of 1.52 (Brindley *et al.*, 1986). Low-temperature FTIR spectra of this sample (Figure 2) revealed that the position of the ν(OH) band of the inner OH group decreased in frequency from 3620 cm^{-1} at 305 K to 3615 cm^{-1} at 15 K. In contrast, the positions of the three ν(OH) bands assigned to the three inner-surface OH groups at 3652, 3669, and 3691 cm^{-1} increased in frequency, upon cooling to 15 K, to 3659, 3678, and 3704 cm^{-1}, respectively. Comparison of the low-temperature FTIR spectra of dickite, which were reported previously in a related study (Bish and Johnston, 1993), with those of kaolinite from the present study found that, in addition to the temperature-induced shifts in position (Figure 3), the widths of the ν(OH) bands decreased

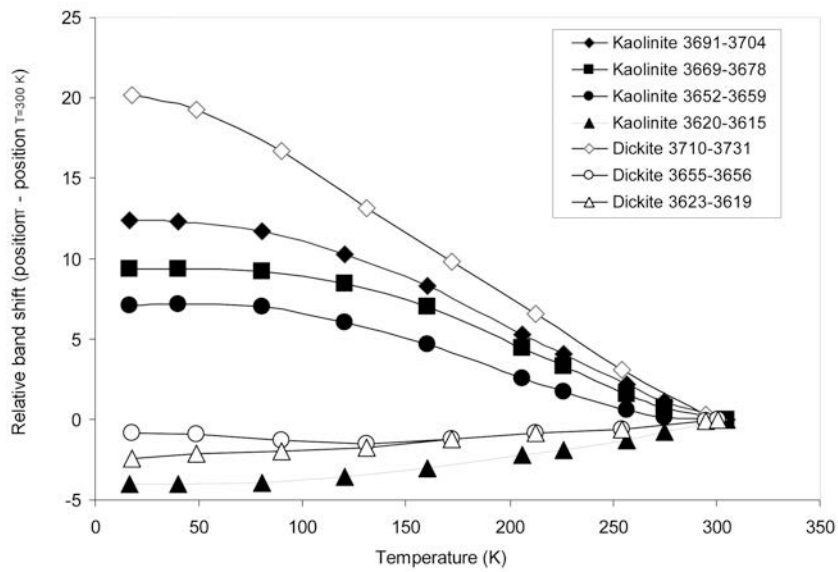

Figure 3. Relative band shift of the ν(OH) bands of kaolinite (Wilkinson County I-B sample; Georgia, USA; closed symbols) and dickite (open symbols) as a function of temperature. The relative band shift corresponds to the position of the band at a given temperature relative to the position of that band at 305 K. (Relative band shift = $(Position_{temp}) - (Position_{T = 305\ K})$). Low-temperature FTIR data for dickite were obtained from an earlier study by Bish and Johnston (1993).

https://doi.org/10.1346/CCMN.2008.0560408 Published online by Cambridge University Press

upon cooling (Figure 4), thereby improving the overall resolution of the ν(OH) region. Although all of the ν(OH) bands narrowed from 300 K to 15 K (Figure 4), the decrease in band width for the 3731 cm^{-1} band (when cooled to 15 K) of dickite was significantly greater compared with the other bands. The influence of temperature (Bish and Johnston, 1993) and pressure (Johnston *et al.*, 2002) on the crystal structures of KGMs is known. For both kaolinite and dickite, most of the thermal contraction occurs along the [001] direction and is primarily due to a decrease in the interlayer separation (Bish, 1993; Bish and Johnston, 1993). This contraction of the interlayer space was reflected by the pronounced frequency shifts and narrowing of the ν(OH) bands assigned to the inner-surface OH groups (Figures 2–4). Similar perturbations of the ν(OH) bands were observed when KGMs were subjected to high pressure. In a recent high-pressure Raman study of dickite, for example, the ν(OH) bands were strongly perturbed under increased pressure (Johnston *et al.*, 2002) and signaled the occurrence of a phase transition at high pressure (Dera *et al.*, 2003).

The space group of kaolinite is *C*1, and the unit cell contains four crystallographically unique OH groups, each having a local site symmetry of 1 (C_1 in Schönflies notation). Due to the low symmetry of kaolinite, all four OH groups are expected to produce distinct ν(OH) stretching bands and each of these bands is both Raman- and IR-active (Johnston *et al.*, 1998). This is consistent with reported IR and Raman spectra of kaolinite, with the possible exception of an additional band observed in both Raman and IR spectra (Johnston *et al.*, 1985; Shoval *et al.*, 1999b). Recently, the complexity of this region observed in Raman and FTIR spectra and the appearance of a fifth ν(OH) band has been attributed to LO-TO splitting (Farmer, 1998; Farmer, 2000; Balan *et al.*, 2001).

Diagnostic ν(OH) bands of kaolinite, dickite, and nacrite

Comparison of the low-temperature FTIR spectrum of kaolinite with the spectra of dickite and nacrite (Figure 5) demonstrated that the ν(OH) bands of the three polytypes are distinct (for comparison, the room temperature FTIR spectra of each polytype are also shown in Figure 5). The low-temperature FTIR spectrum of dickite (Figure 5b) in the OH-stretching region is characterized by three well resolved ν(OH) bands at 3621, 3655, and 3731 cm^{-1}. In previous work, the ν(OH) bands of dickite at 12 K were assigned using time-of-flight neutron powder diffraction data, Rietveld refinement, and low-temperature FTIR methods (Bish and Johnston, 1993). The 3621 cm^{-1} band was assigned to the inner OH group (OH_1); the 3655 cm^{-1} band to OH_2 and OH_4; and the 3731 cm^{-1} band to the OH_3 group. These assignments were later confirmed in a single-crystal Raman study of dickite (Johnston *et al.*, 1998). The spectra shown by traces b and c in Figure 5 show that the OH-stretching bands of kaolinite are distinct from those of dickite and nacrite.

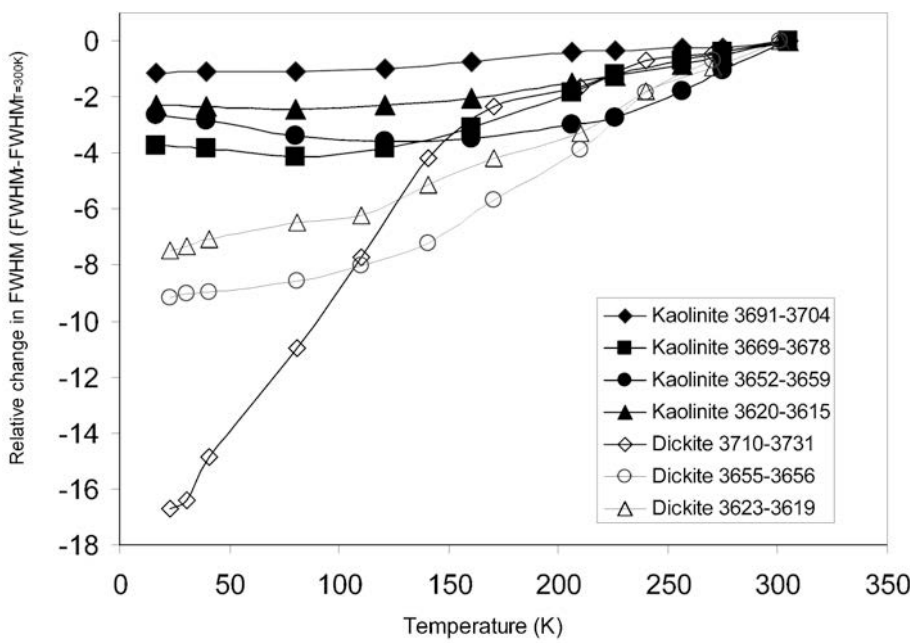

Figure 4. Relative band width (FWHM) of ν(OH) bands of kaolinite (closed symbols) and dickite (open symbols) as a function of temperature. The relative band width corresponds to the full-width-at-half-maximum (FWHM) of the band at a given temperature relative to the FWHM of that band at 305 K. (Relative band width = $(FWHM_T) - (FWHM_{T=305\ K})$). Low-temperature FTIR data for dickite were obtained from an earlier study by Bish and Johnston (1993).

https://doi.org/10.1346/CCMN.2008.0560408 Published online by Cambridge University Press

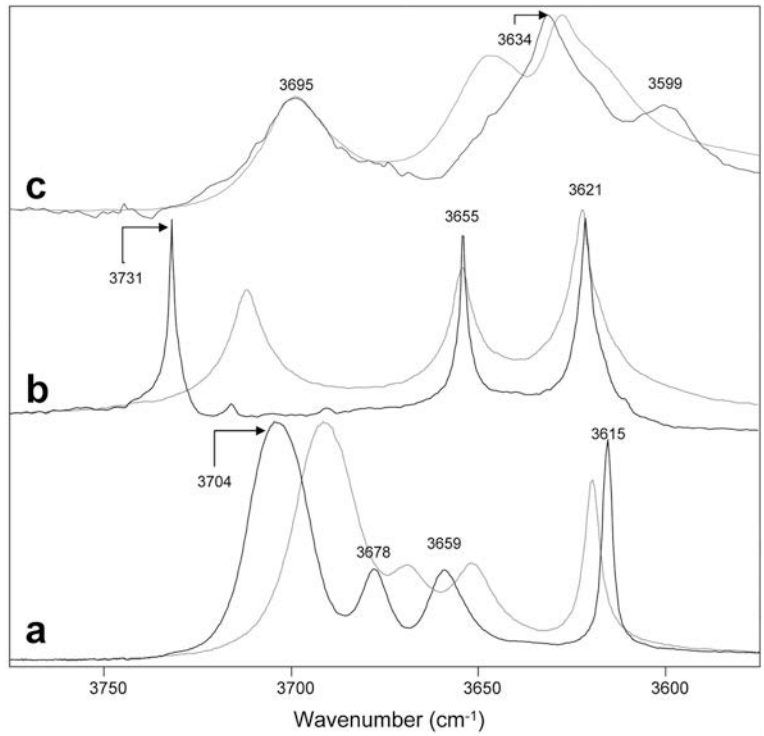

Figure 5. Low-temperature FTIR spectra of kaolinite (a), dickite (b), and nacrite (c) (12–16 K) in the 3750 to 3550 cm^{-1} region. The low-temperature FTIR spectrum of dickite was reported previously by Bish and Johnston (1993). For comparison, the room-temperature FTIR spectra are shown for each KGM in gray.

Using dispersive IR methods, Prost and co-workers observed ν(OH) bands of a nacrite sample cooled to near liquid-helium temperatures at 3597, 3634, and 3693 cm^{-1}, and shoulders at 3713 and 3729 cm^{-1} (Prost *et al.*, 1987). Similar results were obtained for three different nacrite samples using low-temperature (77 K) Raman methods (Frost and Kloprogge, 2000), with bands at 3603–3604, 3621, 3630–3634, and 3697–3700 cm^{-1}. One complication arises in the case of the 3599 cm^{-1} band of nacrite with kaolin samples that contain structural Fe^{3+} substituted for Al^{3+}. In kaolin samples containing large amounts of structural Fe^{3+} (5–10 wt.% as Fe_2O_3), a band at 3598 cm^{-1} is present in the FTIR spectra obtained at room temperature (Iriarte *et al.*, 2005).

A comparison of the low-temperature ν(OH) bands for kaolinite, dickite, and nacrite found in this study with those documented in prior work (Table 2, Figure 5) reveals that low-temperature FTIR spectral analysis of KGMs provides a sensitive method for detecting the presence of kaolinite, dickite, and nacrite. Identification of kaolinite, dickite, and nacrite features is not possible based on FTIR spectra obtained at room temperature. Specifically, the 3731 cm^{-1} band of dickite and the 3599 cm^{-1} band of nacrite are only distinct at low temperature. Furthermore, spectral overlap occurs with the inner OH-stretching bands at 3620 (kaolinite), 3623 (dickite), and 3628 cm^{-1} (nacrite), as well as overlap with the bands at 3650 cm^{-1} (kaolinite), 3655 cm^{-1} (dickite), and 3646 cm^{-1} (nacrite). Upon cooling to low temperature, the bands narrow and shift to positions of minimal overlap.

Correlation of interlayer hydrogen bonding distances with observed ν(OH) band positions

The vacant octahedral site in kaolinite (Figure 1), shown in the [100] projection, is not shifted in one layer relative to the next (Figure 1b). As shown in the [010] projection, the layers are shifted by $a/3$ which minimizes the O-H···O distances (Figure 1b). The corresponding long interlayer hydrogen bond lengths (at 1.5 K) are 3.087, 2.980, and 2.945 Å for H_2, H_3, and H_4, respectively (Table 3; Bish, 1993). In the case of dickite, the vacant octahedral site alternates from the '*B*' site in one layer to the 'C' site in the next layer, using the terminology of Bailey (Bailey, 1963, 1988). A glide plane exists in the dickite [100] projection (Figure 1c). The corresponding long interlayer hydrogen bond lengths for dickite are 2.911, 3.145, and 2.906 Å for H_2, H_3, and H_4, respectively (Table 3; Bish and Johnston, 1993). In the case of nacrite (Figure 1d), the crystallographic *a* and *b* axes are reversed (Zheng and Bailey, 1994). As seen in the [010] projection, one layer is shifted by $b/3$ in successive layers.

The assignments of the observed ν(OH) bands to structural OH groups were based on the interlayer

https://doi.org/10.1346/CCMN.2008.0560408 Published online by Cambridge University Press

Table 2. Low-temperature FTIR band positions of kaolinite, dickite, and nacrite, along with reported literature values.

Kaolinite		Dickite			Nacrite			
This study	Lit(a)	This study	Lit(a)	Lit(b)	This study	Lit(a)	Lit(c)	Diag. bands
					3599	3597	3602	N
3615	3616							K
		3621	3620	3620			3620**	**
					3634	3634	3636	N
		3655	3654	3655				D
3659	3656							K
3678	3679							K
					3695	3694	3697	N
			3685*					*
3704	3711					3713		K
			3716*					*
		3731	3731	3732		3729		D

(a) Prost *et al*. (1989) (band positions corrected by adding 5 cm^{-1}; personal communication)
(b) Bish and Johnston (1993)
(c) Frost and Kloprogge (2000)
* Appear to be trace impurities
** Appears to be a kaolinite or dickite impurity

hydrogen bond distances (Table 3). The longest interlayer OH···O distances correspond to the structural OH groups with the highest energies (*i.e.* frequency) and the weakest participation in hydrogen bonding (Pimentel and McClellan, 1960; Libowitzky, 1999). For kaolinite and dickite, frequencies and ν(OH) positions were available at room temperature and at low temperature. As shown in previous work, the $O\text{-}H_2$ and $O\text{-}H_4$ groups are degenerate (having common interlayer O-H···O distances of 2.91 Å) and are assigned to the 3655 cm^{-1} band (Bish and Johnston, 1993). Similarly, the interlayer hydrogen bond distances for the OH_2···O and OH_4···O groups of nacrite are 2.94 and 2.95 Å and are assigned to the 3650 cm^{-1} band (300 K) (Zheng and Bailey, 1994).

By plotting the positions of the ν(OH) bands *vs*. the corresponding OH···O distances (Figure 6), which apparently are the first detailed correlation of the ν(OH) bands reported for all three polytypes of KGMs, the following points can be derived. First, the frequencies of the ν(OH) bands for all three polytypes are strongly correlated with the OH···O distances (r^2 = 0.92), in agreement with previous work (Johnston *et al.*, 1998; Wang and Johnston, 2000). Second, this linear relationship forms the basis for the utility of low-

Table 3. Structural OH···O distances for kaolinite, dickite, and nacrite at room temperature and low temperature (kaolinite and dickite only) along with assigned OH-stretching vibration based on Bish and Johnston (1993). Structural data for kaolinite were obtained from (Bish and von Dreele, 1989; Bish, 1993); dickite (Joswig and Drits, 1986; Bish and Johnston, 1993); nacrite (Zheng and Bailey, 1994).

		Low-temperature (15 K)		Room-temperature (298 K)	
		OH···O distance (Å)	νOH	OH···O distance (Å)	νOH
Kaolinite	H2	3.087[a]	3704	3.075[b]	3691
	H3	2.980[a]	3678	2.955[b]	3669
	H4	2.945[a]	3659	2.960[b]	3652
Dickite	H2	2.911[c]	3655	2.937[d]	3656
	H3	3.145[c]	3731	3.126[d]	3710
	H4	2.906[c]	3655	2.957[d]	3656
Nacrite	H2			2.951[e]	3650
	H3			3.117[e]	3705
	H4			2.944[e]	3650

[a] Bish (1993)
[b] Bish and von Dreele (1989)
[c] Bish and Johnston (1993)
[d] Joswig and Drits (1986)
[e] Zheng and Bailey (1994)

https://doi.org/10.1346/CCMN.2008.0560408 Published online by Cambridge University Press

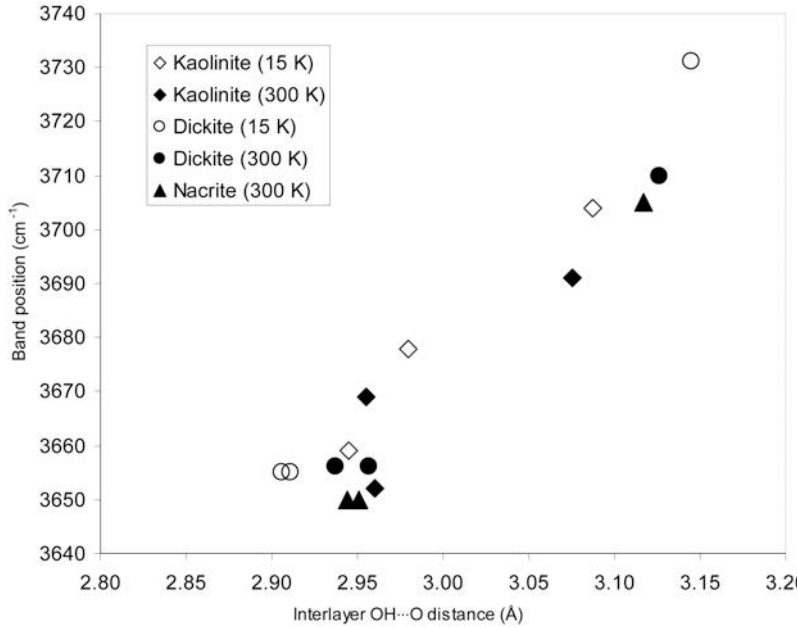

Figure 6. Band positions of the ν(OH) bands of kaolinite, dickite, and nacrite plotted *vs*. their interlayer O–H···O distances. In the case of kaolinite and dickite, room-temperature and low-temperature (T = 15 K) data were available; only room-temperature data were available for nacrite. The data used to construct this figure are given in Table 3.

temperature FTIR as a means of studying structural disorder in KGMs. Each of the three polytypes is characterized by a unique set of interlayer hydrogen bond distances. As the data in Figure 5 show, each polytype is characterized by a unique set of ν(OH) bands in the low-temperature FTIR spectra.

The ν(OH) region of KGMs has been the subject of detailed analysis by numerous investigators and some disagreement exists among them regarding the assignment of the bands. Although a linear relationship exists between band positions of the interlayer OH groups and their corresponding interlayer OH···O distances at the global scale (comparison of all three polytypes), scatter is clearly present in the data, which can be attributed, in part, to the following. First, several experimental and theoretical studies have shown that the three high-frequency bands in the spectrum of kaolinite correspond to the coupled motion of inner-surface OH groups (e.g. (Rouxhet *et al.*, 1977; Farmer, 1998; Balan *et al.*, 2001). In addition, effects due to LO-TO splitting have been reported for kaolinite and dickite (Farmer, 1998; Farmer, 2000; Balan *et al.*, 2001; Balan *et al.*, 2005) and LO-TO splitting also likely occurs in nacrite. The effect is a band shift related to the electrostatic charges occurring at the surface of the polarized dielectric particles. For platy crystals, bands at the TO and LO frequencies can be resolved (Farmer, 1998; Farmer, 2000). However, a distribution of band positions resulting from the corresponding depolarization field is expected when particles are not ellipsoidal or when various particle shapes occur in the sample. Although relatively minor, coupling and LO-TO splitting effects contribute to the scatter shown in Figure 6. One final source of scatter is that the vibrational and structural data were not obtained on the same sample or under the same conditions.

Low-temperature FTIR spectra of high-HI kaolinites

Low-temperature FTIR spectra of two high-HI kaolins are shown in Figure 7. Keokuk kaolinite is generally recognized as one of the most ordered kaolin-

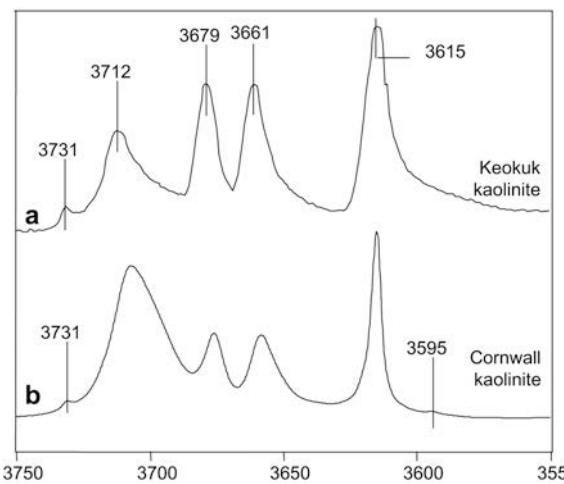

Figure 7. Low-temperature FTIR spectra of kaolins from hydrothermal origin in the 3750 to 3550 cm^{-1} region. The broadened bands present in the low-temperature FTIR spectrum of the Keokuk kaolinite sample are attributed to the large particle size of this material. The position of the inner-surface OH band at 3712 to 3702 cm^{-1} varies and depends on the size and shape of the kaolinite particles.

https://doi.org/10.1346/CCMN.2008.0560408 Published online by Cambridge University Press

ite samples available. This sample, kindly provided by W.D. Keller, formed in a geode and was described by Keller (1977). Upon cooling to 12 K, ν(OH) bands were observed at 3615, 3661, 3679, 3712, and 3731 cm^{-1}. In comparison with other, less well ordered kaolins, the larger FWHM of these bands and the high asymmetry of the 3712 cm^{-1} band are due to the large particle size of the Keokuk kaolinite sample. Vibrational spectra of KGMs in the ν(OH) region are sensitive to particle-size effects, and when the average particle size is similar to the wavelength of the IR radiation (2.5−25 μm), spectral distortions and line-broadening occur (Prost, 1973; Farmer, 1974; Johnston and Aochi, 1996). The 3704−3712 cm^{-1} band (low-temperature band positions) of kaolinite, in particular, has been shown to be sensitive to particle-size effects and the type of spectroscopic method (Johnston *et al.*, 1998; Shoval *et al.*, 1999a; Shoval *et al.*, 1999b; Farmer, 2000). Of particular interest in this study is the presence of the 3731 cm^{-1} band. This ν(OH) band is unique to dickite (Figure 5) and provides unambiguous evidence that dickite and/or dickite-like stacking sequences are present in this sample. The low-temperature FTIR spectra of the Keokuk and Cornwall kaolinite specimens are both characterized by this dickite feature at ~3731 cm^{-1}. Unclear from the low-temperature FTIR spectra, however, is whether this spectral feature is due to discrete dickite particles or to dickite-like stacking sequences, analogous to illite-smectite interstratification. However, previous XRD studies have documented the existence of several percent of discrete dickite in the Keokuk kaolin (Bish and von Dreele, 1989). A weak band at 3595 cm^{-1} is observed in the Cornwall sample.

High-HI secondary kaolins

Low-temperature FTIR spectra of high-HI secondary kaolins from Georgia (a) and Brazil (b) are shown in Figure 8. With the exception of the Wilkinson County sample, all of these high-HI kaolins contain dickite and nacrite features as demonstrated by the bands at 3731 (D), 3655 (D), 3634 (N), and 3599 (N) cm^{-1}. Similar to the low-temperature FTIR spectra of the Keokuk and Cornwall kaolins, three of the four high-HI kaolin samples contain clearly discernible dickite and nacrite features in their spectra. Dickite features are evidenced by the well resolved bands at 3731 cm^{-1} and by the 3655 cm^{-1} band. Nacrite features at 3599 and 3634 cm^{-1} are present in spectra of the Washington County, Capim, and Patinga samples. X-ray diffraction analyses did not detect the presence of either dickite or nacrite in these samples. However, the ability of XRD to detect trace to low-levels of dickite and nacrite in poorly-ordered kaolinite samples is limited.

According to Plançon *et al*. (1989) and Plançon and Zacharie (1990), the predominant type of structural disorder in KGMs is the occurrence of a translation between adjacent layers of approximately $-a/3+b/3$ (not the typical $-a/3$ translation) and the existence of layers having a vacant C octahedral site. In addition, apparently small displacements of one layer with respect to an adjacent layer may occur as a result of the broad potential energy minimum in layer stacking energy

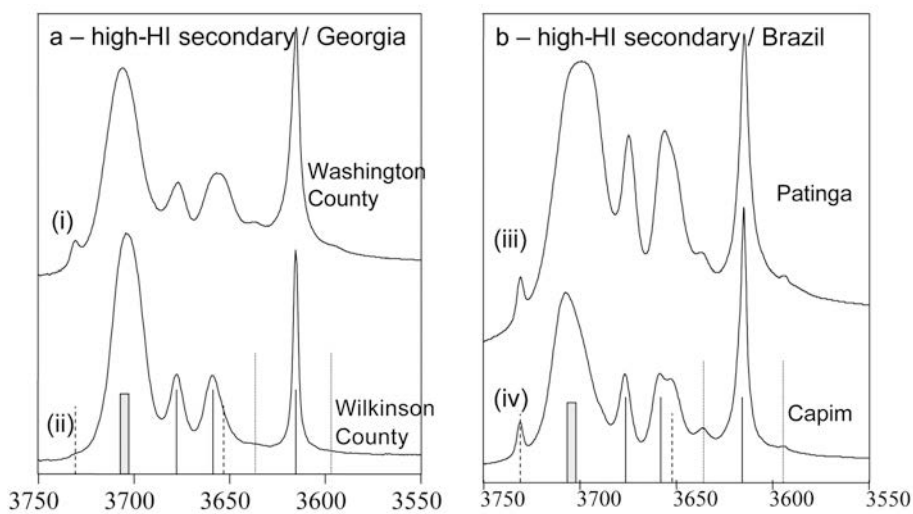

Figure 8. Low-temperature FTIR spectra of high-HI kaolins of sedimentary origin. The spectra on the left side of the figure are from Georgia. On the right are two high-HI kaolins from Brazil (Patinga and Capim). In the case of the Wilkinson County sample, only four OH-stretching bands are present and there is no evidence for the presence of dickite or nacrite in this specimen. In the Washington County specimen, however, the band at 3731 cm^{-1} clearly indicates the presence of dickite and the band at 3634 cm^{-1} reflects the possible occurrence of nacrite. As shown in the Brazilian kaolins, the presence of these solid phases is pronounced. In the spectrum of the Capim sample, the bands at 3731 and 3655 cm^{-1} are assigned to dickite. In addition, the bands at 3595 and 3634 cm^{-1} are assigned to nacrite. The solid lines correspond to kaolinite, dashed lines to dickite, and dotted lines to nacrite.

https://doi.org/10.1346/CCMN.2008.0560408 Published online by Cambridge University Press

(Giese, 1982; Plançon and Zacharie, 1990). For example, in kaolinite where the vacant octahedral site is normally in the 'B' position, disorder would be introduced whenever a mistake occurs in the location of the vacant octahedral site, for example in a layer containing one or more 'C' site vacancies. In other words, a dickite-like component is introduced into the kaolinite crystal (Brindley and Porter, 1978). Every other layer in nacrite is rotated 180º and the octahedral vacancy rotates ±60º between layers, giving nacrite a two-layer structure (Bailey, 1988). As discussed previously, Kogure and Inoue (2005a, 2005b) directly observed disorder of octahedral vacant sites in a hydrothermal kaolin sample using HRTEM.

Low-HI kaolins

Low-temperature FTIR spectra of low-HI secondary kaolins are shown in Figure 9. Kaolinite, dickite, and nacrite signatures are present in all three samples. The presence of dickite and nacrite features may support the earlier suggestion of Farmer and Russel (1964) and Lombardi et al. (1987) that layer stacking faults are the predominant type of structural disorder occurring in poorly ordered kaolins. However, the spectra may also indicate the presence of discrete dickite and nacrite. In either case, these spectra provide unambiguous evidence that both dickite and nacrite polytypes or dickite- and nacrite-like stacking sequences are present in these poorly ordered kaolins.

Influence of particle size

To better understand the relationship of the ν(OH) bands with particle size and shape, low-temperature FTIR spectra of three different particle size fractions (5−2 μm, 2.0−0.5 μm, and <0.2 μm) of the Capim kaolin were measured (Figure 10). Kaolinite, dickite, and nacrite features are present in all three size fractions, but the distribution of these features does not appear to be uniform among the different size fractions. In particular, the relative intensity of the nacrite component at 3634 cm^{-1} is increased in the <0.2 μm fraction. The dickite features at 3731 and 3655 cm^{-1} are present in all three size fractions but these spectral features are better resolved in the 5−2 μm size fraction. These data suggest that the distribution of kaolinite-, dickite-, and nacrite-like features observed using low-temperature FTIR spectroscopy can provide a useful diagnostic method to probe the crystal chemistry, structural disorder, and genesis of kaolin-group minerals.

Because of the well resolved, pronounced dickite- and nacrite-like features in the Capim sample, this sample was investigated further using SAED. No HRTEM analysis of the Capim sample was possible because of the small particle size and because it was susceptible to beam damage. However, obtaining SAED patterns of this sample was possible (Figure 11a, taken along one of the Y_i directions (Bailey, 1988)). The reciprocal lattice rows in the pattern were streaked along

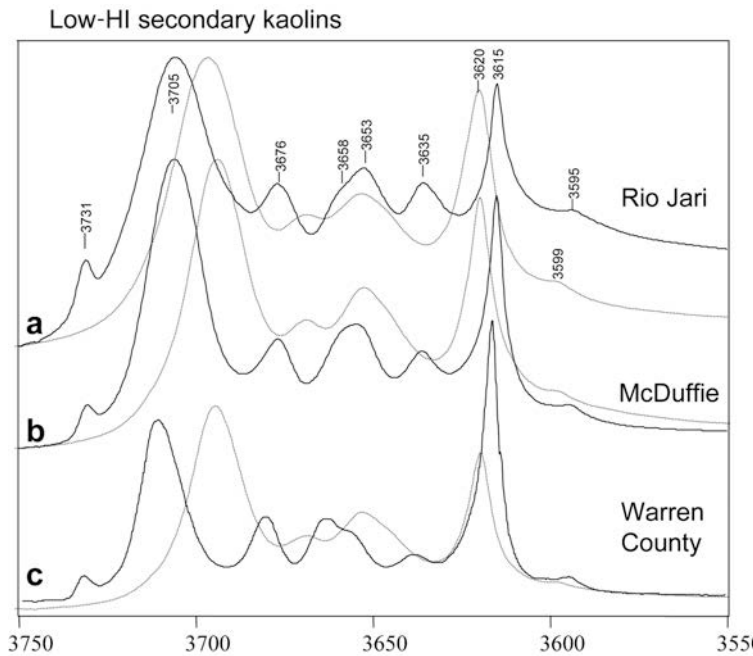

Figure 9. Low-temperature FTIR spectra of low-HI kaolins of sedimentary origin. The two lower spectra correspond to kaolins from Georgia and the uppermost trace is of a kaolin sample from Brazil (Rio Jari). For comparison, room-temperature FTIR spectra are plotted in gray.

https://doi.org/10.1346/CCMN.2008.0560408 Published online by Cambridge University Press

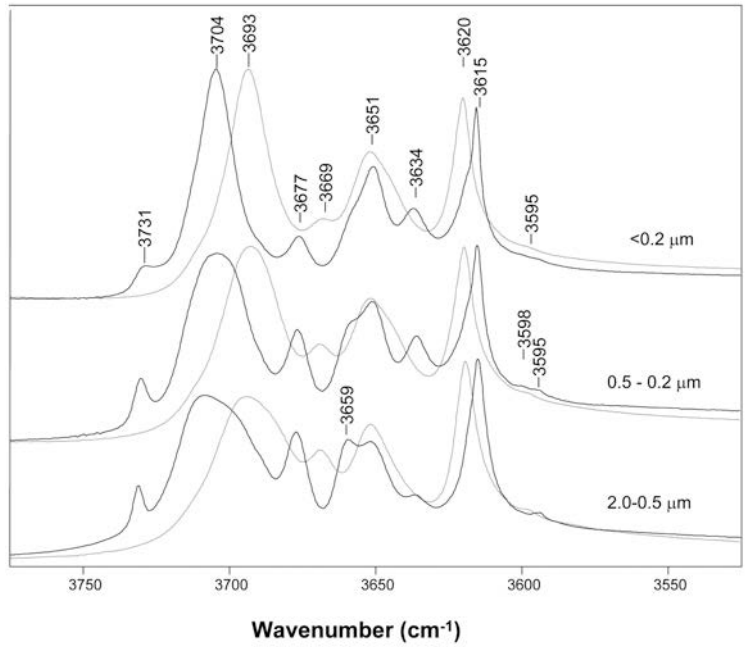

Figure 10. Low-temperature FTIR spectra of three size fractions of the Capim kaolin from Brazil (high-HI kaolin of sedimentary origin). For comparison, room-temperature FTIR spectra are plotted in gray.

the c^* direction, indicating that this crystal contained a mixture of stacking sequences from different subfamilies of 1:1 phyllosilicates (Bailey, 1988; Kogure *et al.*, 2001). For comparison, similar electron diffraction images of a kaolin specimen from a hydrothermal deposit (Kasuga mine, Japan) are shown in Figure 11b (Kogure and Inoue, 2005b). Analysis by HRTEM of this specimen found that the crystal from which the patterns were obtained contained disorder of B and C layers and disorder of interlayer translations (Figure 5; Kogure and Inoue, 2005b). However, the diffraction pattern along Y_i directions was perfectly discrete (Figure 11b). This is because kaolinite, its enantiomer, and dickite belong to the same subfamily (subfamily A) (Bailey, 1988). In other words, the streaked pattern in Figure 11a strongly suggests the intergrowth of nacrite (subfamily D) and kaolinite-dickite within a single crystal.

DISCUSSION

The presence of kaolinite, dickite, and nacrite polytype features are clearly resolved in low-tempera-

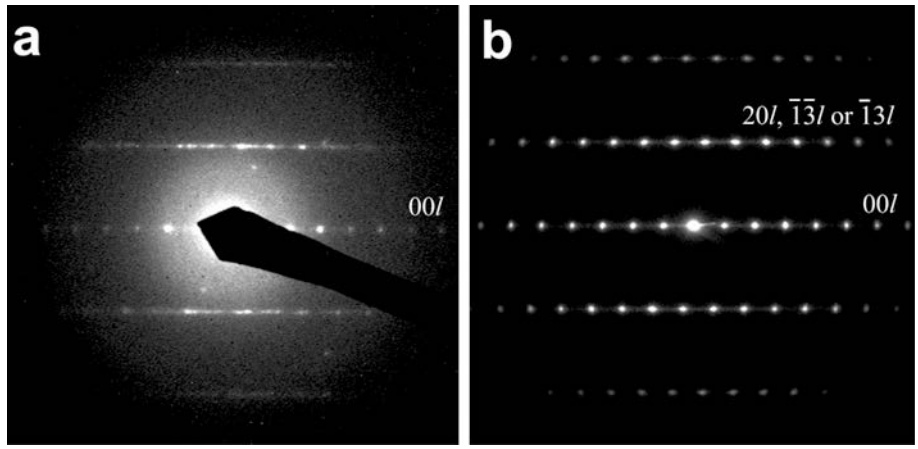

Figure 11. (a) Selected-area electron diffraction (SAED) pattern along one of the Y_i directions from the Capim kaolin, showing an interstratification of different subfamilies, supposedly nacrite (subfamily D) and kaolinite-dickite (subfamily A). (b) SAED pattern along the same direction, from a hydrothermal kaolin from Kasuga mine, Japan (Kogure and Inoue, 2005b). In this case the stacking is the mixture of kaolinite and dickite that belong to the same subfamily and the diffraction is discrete, which corresponds to a 0.7 nm periodicity.

https://doi.org/10.1346/CCMN.2008.0560408 Published online by Cambridge University Press

ture FTIR spectra of a diverse suite of samples ranging from well ordered to highly disordered kaolins. Whether these features are from discrete phases or from interstratification of dickite and/or nacrite stacking sequences within a given crystal cannot be resolved solely on the basis of the low-temperature FTIR spectra. However, the electron diffraction image obtained from the Capim sample (Figure 11) provides strong support for the presence of interstratified layers of dickite and nacrite in a given kaolinite crystal. Although discrete, well ordered dickite is often associated with hydrothermal deposits and burial diagenesis of sandstones (Bayliss *et al.*, 1965; Ehrenberg *et al.*, 1993; Lanson *et al.*, 1996; Cruz and Reyes, 1998; Beaufort *et al.*, 1998; Lanson *et al.*, 2002), the origin of the Capim kaolin, along with the secondary kaolins from Georgia, is not hydrothermal.

In general, the appearance and growth of the dickite and nacrite features increase with increasing disorder and this is particularly true for the sedimentary kaolins from Brazil and the low-HI kaolins from Georgia. The ability to resolve these features at low temperature is based on the well defined ν(OH) features of the three polytypes that develop when cooled below 50 K. The ν(OH) band of dickite assigned to the OH_3 group (3731 cm−1) (Bish and Johnston, 1993) is of particular interest. The position of this band increased in frequency by 20 cm^{-1} (Figure 3) and the FWHM decreased by 17 cm^{-1} (Figure 4) and can only be fully resolved when cooled to T<30 K. Although several studies reported FTIR spectra of individual polytypes obtained at liquid N_2 temperatures (77 to 100 K) (Frost and Kloprogge, 2000) and of disordered kaolins (Brindley *et al.*, 1986), spectra obtained at these intermediate temperatures do not show the full potential that can be realized by cooling to near liquid He temperatures (~15 K).

The assignment of the low-temperature features to dickite-like features is unambiguous, based on the well resolved spectral features that appear at low temperature and on the fact that the three polytypes have unique interlayer OH···O distances. Low-temperature features consistent with the presence of nacrite also appear in disordered kaolin samples based on the presence of a band at 3635 cm^{-1}. Although the low-temperature FTIR spectrum of pure nacrite has a band at 3599 cm^{-1}, the 3599−3595 cm^{-1} band present in the low-temperature FTIR spectra of disordered kaolin samples (*e.g.* Figure 9) may be due to nacrite-like stacking sequences and/or to the presence of structural Fe^{3+}. A weak band is present in the room temperature FTIR spectra of these samples, in agreement with previous IR studies of disordered kaolins containing large amounts of Fe^{3+} (Iriarte *et al.*, 2005). For the low-temperature FTIR spectra of the low-HI kaolins (Figure 9), the bands are somewhat broader and some variations are observed in the intensity of the 3634 and 3599 cm^{-1} features. Furthermore, the 3634 cm^{-1} band in the <0.2 μm size fraction of the Capim kaolin sample has maximum intensity but the 3599 cm^{-1} band is unresolved or possibly too broad (Figure 10). Whether these features are from discrete or interstratified layers cannot be resolved on the basis of the low-temperature FTIR spectra alone. However, SAED patterns of the Capim sample indicated that the dickite- and nacrite-like features seen in FTIR spectra of this sample are due to interstratification within a given crystal. In this context, the low-temperature FTIR method is a powerful new tool to characterize various types of structural disorder in KGMs. Further, this method will potentially extend our understanding of structural disorder in kaolin group minerals as a method complementary to widely established XRD-based methods such as the HI.

Kaolins from hydrothermal deposits are known to contain discrete dickite, depending on the temperature and depth of the deposit. This may be the case for the observation of dickite in the Cornwall and Keokuk kaolins (Figure 7). Some debate continues as to the thermodynamic stability of these polytypes. Thermochemical measurements of kaolinite, dickite, and nacrite (de Ligny and Navrotsky, 1999; Fialips *et al.*, 2001) have shown that kaolinite has the lowest enthalpy of formation, indicating that dickite and nacrite are less stable than kaolinite and are metastable phases under surface conditions. On the other hand, recent first-principle theoretical studies (Benco *et al.*, 2001a; Sato *et al.*, 2004; Balan *et al.*, 2005) have shown that the overall energetics among the three polytypes are very similar. In addition, experimental solubility measurements (Zotov *et al.*, 1998) also suggest that the difference in Gibbs free energy between kaolinite and dickite is significantly smaller than that obtained from high-T calorimetric measurements. Based on the observed transformation of kaolinite to dickite with increasing temperature and pressure in burial diagenesis, some authors have argued that kaolinite is the metastable phase. These questions cannot be resolved here. However, observed with interest is the presence of dickite- and nacrite-like features in disordered kaolin samples of low-temperature origin. These observations are also consistent with formation of a disordered dickite in Jamaica, also of low-temperature origin (Brindley and Porter, 1978). The presence of dickite and nacrite spectral features in such a diverse group of kaolin samples as analyzed in this paper of different geological origins suggests that differences in the thermodynamic stability between the three polytypes is small.

CONCLUSION

The FTIR spectra of a diverse group of kaolin samples analyzed at low temperature (~15 K) revealed surprisingly well resolved bands in the ν(OH) region from 3750 to 3550 cm^{-1}. Comparison of these spectra with those obtained for 'pure' well ordered kaolinite, dickite, and nacrite specimens enabled the unambiguous

https://doi.org/10.1346/CCMN.2008.0560408 Published online by Cambridge University Press

identification of kaolinite, dickite, and nacrite features. Assignments were confirmed based on the linear relationship between the positions of ν(OH) bands of the three polytypes at low and room temperature and known interlayer OH···O distances. Only one kaolin sample, from Wilkinson County, Georgia (Figure 8), contained only kaolinite features. All other kaolin samples analyzed revealed the presence of dickite- and, in some cases, nacrite-like features, including the high-HI kaolins obtained from geodes (Keokuk, Iowa, USA), a primary kaolin (Cornwall, UK), and a high-HI secondary kaolin from Brazil (Capim). In general, the overall contribution of dickite and nacrite features increased as disorder increased, which may be consistent with the statistical possibility of having non-kaolinite stacking sequences. In addition, the relative proportion of kaolinite, dickite, and nacrite features in a given sample showed variation with particle size. The low-temperature FTIR method is unable to fully resolve the question as to whether the dickite and nacrite features are due to stacking mistakes or to the presence of discrete polytypes in the sample. However, electron diffraction patterns obtained from one sample (Capim) provided direct evidence that dickite- and nacrite-like stacking sequences were present in one crystallite as opposed to existing as discrete dickite and nacrite particles in the sample. The results presented here provide a new means of assessing structural disorder and of determining the presence of small amounts of dickite- and nacrite-like stacking sequences in kaolin samples based on the improved spectral resolution of kaolin samples observed at low temperature (<15 K).

ACKNOWLEDGMENTS

The authors thank Associate Editor, Bruno Lanson, and three reviewers, including Sabine Petit, who provided detailed review comments which were helpful in improving the manuscript.

REFERENCES

Bailey, S.W. (1963) Polymorphism of the kaolin minerals. *American Mineralogist*, **48**, 1196–1209.

Bailey, S.W. (1988) Polytypism of 1-1 layer silicates. Pp. 9–27 in: *Hydrous Phyllosilicates (exclusive of Micas)* (S.W. Bailey, editor). Reviews in Mineralogy, **19**. Mineralogical Society of America, Washington, D.C.

Balan, E., Saitta, A.M., Mauri, F., and Calas, G. (2001) First-principles modeling of the infrared spectrum of kaolinite. *American Mineralogist*, **86**, 1321–1330.

Balan, E., Lazzeri, M., Saitta, A.M., Allard, T., Fuchs, Y., and Mauri, F. (2005) First-principles study of OH-stretching modes in kaolinite, dickite, and nacrite. *American Mineralogist*, **90**, 50–60.

Barrios, J., Plançon, A., Cruz, M.I., and Tchoubar, C. (1977) Qualitative and quantitative study of stacking faults in a hydrazine treated kaolinite. Relationship with the infrared spectra. *Clays and Clay Minerals*, **25**, 422–429.

Bayliss, P., Loughnan, F.C., and Standard, J.C. (1965) Dickite in Hawkesbury Sandstone of Sydney Basin Australia. *American Mineralogist*, **50**, 418–426.

Beaufort, D., Cassagnabere, A., Petit, S., Lanson, B., Berger, G., Lacharpagne, J.C., and Johansen, H. (1998) Kaolinite-to-dickite reaction in sandstone reservoirs. *Clay Minerals*, **33**, 297–316.

Benco, L., Tunega, D., Hafner, J., and Lischka, H. (2001a) Ab initio density functional theory applied to the structure and proton dynamics of clays. *Chemical Physics Letters*, **333**, 479–484.

Benco, L., Tunega, D., Hafner, J., and Lischka, H. (2001b) Orientation of OH groups in kaolinite and dickite: Ab initio molecular dynamics study. *American Mineralogist*, **86**, 1057–1065.

Bish, D.L. (1993) Rietveld Refinement of the kaolinite structure at 1.5 K. *Clays and Clay Minerals*, **41**, 738–744.

Bish, D.L. and Chipera, S.J. (1998) Proceedings of the 35th Annual Clay Minerals Society Meeting, Cleveland, OH 90 (abstract).

Bish, D.L. and Chipera, S.J. (1999) Euroclay 1999: Conference of the European Clay Groups Association, September 5–9, 1999, 64 (abstract).

Bish, D.L. and Johnston, C.T. (1993) Rietveld refinement and Fourier transform infrared spectroscopic study of the dickite structure at low temperature. *Clays and Clay Minerals*, **41**, 297–304.

Bish, D.L. and von Dreele, R.B. (1989) Rietveld refinement of non-hydrogen atomic positions in kaolinite. *Clays and Clay Minerals*, **37**, 289–296.

Bookin, A.S., Drits, V.A., Plançon, A., and Tchoubar, C. (1989) Stacking faults in kaolin-group minerals in the light of real structural features. *Clays and Clay Minerals*, **37**, 297–307.

Brindley, G.W. and Porter, A.R.D. (1978) Occurrence of dickite in Jamaica – ordered and disordered varieties. *American Mineralogist*, **63**, 554–562.

Brindley, G.W., Kao, C., Harrison, J.L., Lipsicas, M., and Raythatha, R. (1986) Relation between structural disorder and other characteristics of kaolintes and dickites. *Clays and Clay Minerals*, **34**, 239–249.

Buatier, M.D., Deneele, D., Dubois, M., Potdevin, J.L., and Lopez, M. (2000) Nacrite in the Lodeve Permian Basin: a TEM and fluid-inclusion study. *European Journal of Mineralogy* **12**, 329–340.

Cruz, M.D.R. and Reyes, E. (1998) Kaolinite and dickite formation during shale diagenesis: isotopic data. *Applied Geochemistry*, **13**, 95–104.

de Ligny, D. and Navrotsky, A. (1999) Energetics of kaolin polymorphs. *American Mineralogist*, **84**, 506–516.

Dera, P., Prewitt, C.T., Japel, S., Bish, D.L., and Johnston, C.T. (2003) Pressure-controlled polytypism in hydrous layered materials. *American Mineralogist*, **88**, 1428–1435.

Dominy, S.C. and Camm, G.S. (1998) Geology and hydrothermal development of Bostraze-Balleswidden kaolin deposit, Cornwall, United Kingdom. *Transactions of the Institution of Mining and Metallurgy Section B – Applied Earth Science*, **107**, B148–B157.

Dornberger-Schiff, K. and Ďurovič, S. (1975) OD-interpretation of kaolinite-type structures. 1. Symmetry of kaolinite packets and their stacking possibilities. *Clays and Clay Minerals*, **23**, 219–229.

Ehrenberg, S.N., Aagaard, P., Wilson, M.J., Fraser, A.R., and Duthie, D.M.L. (1993) Depth-dependent transformation of kaolinite to dickite in sandstones of the Norwegian Continental Shelf. *Clay Minerals*, **28**, 325–352.

Farmer, V.C. (1974) *The Infrared Spectra of Minerals.* Mineralogical Society, London, 539 pp.

Farmer, V.C. (1998) Differing effects of particle size and shape in the infrared and Raman spectra of kaolinite. *Clay Minerals*, **33**, 601–604.

Farmer, V.C. (2000) Transverse and longitudinal crystal modes

associated with OH-stretching vibrations in single crystals of kaolinite and dickite. *Spectrochimica Acta Part A – Molecular and Biomolecular Spectroscopy*, **56**, 927–930.

Farmer, V.C. and Russell, J.D. (1964) The infra-red spectra of layer silicates. *Spectrochimica Acta*, **20**, 1149–1173.

Fialips, C.I., Navrotsky, A., and Petit, S. (2001) Crystal properties and energetics of synthetic kaolinite. *American Mineralogist*, **86**, 304–311.

Fialips, C.I., Majzlan, J., Beaufort, D., and Navrotsky, A. (2003) New thermochemical evidence on the stability of dickite vs. kaolinite. *American Mineralogist*, **88**, 837–845.

Frost, R.L. and Kloprogge, J.T. (2000) Raman spectroscopy of nacrite single crystals at 298 and 77K. *Spectrochimica Acta Part A – Molecular and Biomolecular Spectroscopy*, **56**, 931–939.

Giese, R.F. (1973) Interlayer bonding in kaolinite, dickite, nacrite. *Clays and Clay Minerals*, **21**, 145–149.

Giese, R.F. (1982) Theoretical studies of the kaolin minerals: electrostatic calculations. *Bulletin of Mineralogy*, **105**, 417–424.

Giese, R.F. (1990) Kaolin minerals: structures and stabilities. Pp 29–66 in: *Hydrous Phyllosilicates (exclusive of Micas)* (S.W. Bailey, editor). Reviews in Mineralogy, **19**. Mineralogical Society of America, Washington D.C.

Giese, R.F. and Datta, P. (1973) Hydroxyl orientation in kaolinite, dickite, and nacrite. *American Mineralogist*, **58**, 471–479.

Hendricks, S.B. (1938) The crystal structure of nacrite Al2O3 2SiO2 2H2O and the polymorphism of the kaolin minerals. *Zeitschrift für Kristalographie*, **100**, 509–518.

Hinckley, D.N. (1963) Variability in crystallinity values among the kaolin deposits of the coastal plain of Georgia and South Carolina. *Clays and Clay Minerals*, **11**, 229–235.

Iriarte, B., Petit, S., Huertas, F.J., Fiore, S., Grauby, O., Decarreau, A., and Linares, J. (2005) Synthesis of kaolinite with a high level of Fe^{3+} for A1 substitution. *Clays and Clay Minerals*, **53**, 1–10.

Johnston, C.T. and Aochi, Y.O., (1996) Fourier transform infrared and Raman spectroscopy. Pp. 269–321 in: *Methods of Soil Analysis Part 3 – Chemical Methods* (D.L. Sparks, editor). Soil Science Society of America, Madison, Wisconsin.

Johnston, C.T., Agnew, S.F., and Bish, D.L. (1990) Polarized single-crystal Fourier-transform infrared microscopy of Ouray dickite and Keokuk kaolinite. *Clays and Clay Minerals*, **38**, 573–583.

Johnston, C.T., Helsen, J., Schoonheydt, R.A., Bish, D.L., and Agnew, S.F. (1998) Single crystal Raman spectroscopic study of dickite. *American Mineralogist*, **83**, 75–84.

Johnston, C.T., Sposito, G., and Birge, R.R. (1985) Raman spectroscopic study of kaolinite in aqueous suspension. *Clays and Clay Minerals*, **33**, 483–489.

Johnston, C.T., Wang, S.L., Bish, D.L., Dera, P., Agnew, S.F., and Kenney, J.W. (2002) Novel pressure-induced phase transformations in hydrous layered materials. *Geophysical Research Letters*, **29**, art. 1770.

Joswig, W. and Drits, V.A. (1986) The orientation of the hydroxyl groups in dickite by X-ray diffraction. *Neues Jahrbuch für Mineralogie Monatshefte*, 19–22.

Keller, W.D. (1977) Scan electron micrographs of kaolins collected from diverse environments of origin – IV. Georgia kaolin and kaolinizing source rocks. *Clays and Clay Minerals*, **25**, 311–345.

Keller, W.D. and Haenni, R.P. (1978) Effects of micro-sized mixtures of kaolin minerals on properties of kaolinites. *Clays and Clay Minerals*, **26**, 384–396.

Kogure, T. and Inoue, A. (2005a) Determination of defect structures in kaolin minerals by high-resolution transmission electron microscopy (HRTEM). *American Mineralogist*, **90**, 85–89.

Kogure, T. and Inoue, A. (2005b) Stacking defects and long-period polytypes in kaolin minerals from a hydrothermal deposit. *European Journal of Mineralogy*, **17**, 465–473.

Kogure, T., Hybler, J., and Ďurovič, S. (2001) A HRTEM study of cronstedtite: Determination of polytypes and layer polarity in trioctahedral 1:1 phyllosilicates. *Clays and Clay Minerals*, **49**, 310–317.

Lanson, B., Beaufort, D., Berger, G., Baradat, J., and Lacharpagne, J.C. (1996) Illitization of diagenetic kaolinite-to-dickite conversion series: Late-stage diagenesis of the Lower Permian Rotliegend sandstone reservoir, offshore of the Netherlands. *Journal of Sedimentary Research*, **66**, 501–518.

Lanson, B., Beaufort, D., Berger, G., Bauer, A., Cassagnabere, A., and Meunier, A. (2002) Authigenic kaolin and illitic minerals during burial diagenesis of sandstones: a review. *Clay Minerals*, **37**, 1–22.

Ledoux, R.L. and White, J.L. (1964) Infrared study of selective deuteration of kaolinite and halloysite at room temperature. *Science*, **145**, 47–49.

Libowitzky, E. (1999) Correlation of O-H stretching frequencies and O-H···O hydrogen bond lengths in minerals. *Monatshefte für Chemie*, **130**, 1047–1059.

Lombardi, G., Russell, J.D., and Keller, W.D. (1987) Compositional and structural variations in the size fractions of a sedimentary and a hydrothermal kaolin. *Clays and Clay Minerals*, **35**, 321–335.

Michaelian, K.H. (1986) The Raman spectrum of kaolinite #9 at 21 deg. C. *Canadian Journal of Chemistry*, **64**, 285–289.

Moore, D.M. and Reynolds, R.C. (1989) *X-ray Diffraction and the Identification and Analysis of Clay Minerals*. Oxford University Press, Oxford, UK, 332 pp.

Murray, H.H. (1954) Structural variations of some kaolinites in relation to dehydrated halloysite. *American Mineralogist*, **39**, 97–108.

Pimentel, G.C. and McClellan, A.B. (1960) *The Hydrogen Bond*, 1st edition. W.H. Freeman and Co., San Fransisco, USA, 475 pp.

Plançon, A. (2001) Order-disorder in clay mineral structures. *Clay Minerals*, **36**, 1–14.

Plançon, A. and Tchoubar, C. (1977) Determination of structural defects in phyllosilicates by X-ray powder diffraction – II. Nature and proportion of defects in natural kaolinites. *Clays and Clay Minerals*, **25**, 436–450.

Plançon, A. and Zacharie, C. (1990) An expert system for the structural characterization of kaolinites. *Clay Minerals*, **25**, 249–260.

Plançon, A., Giese, R.F., and Snyder, R. (1988) The Hinckley index for kaolinites. *Clay Minerals*, **23**, 249–260.

Plançon, A., Giese, R.F., Snyder, R., Drits, V.A., and Bookin, A.S. (1989) Stacking faults in the kaolin-group minerals – defect structures of kaolinite. *Clays and Clay Minerals*, **37**, 203–210.

Post, J.E. and Bish, D.L. (1989) Rietveld refinement of crystal structures using powder X-ray diffraction data. Pp. 277–305 in: *Modern Powder Diffraction.* (D.L. Bish and J.E. Post, editors). Reviews in Mineralogy, **20**. Mineralogical Society of America, Washington D.C.

Prost, R. (1973) The influence of the christiansen effect on the I.R. spectra of powders. *Clays and Clay Minerals*, **21**, 363–368.

Prost, R. (1984a) Etude par spectroscopie infrarouge a basse temperature des groupes OH de structure de la kaolinite, de la dickite et de la nacrite. *Agronomie*, **4**, 403–406.

Prost, R. (1984b) Low temperature IR study of structural OH groups of kaolinite, dickite and nacrite. *Agronomie*, **4**, 403–406.

Prost, R., Dameme, A., Huard, E., and Driard, J. (1987) Low temperature (300-5K) IR study of structural OH groups of

kaolinite, dickite, and nacrite. Pp. 17–23 in: *Proceedings of the International Clay Conference, Denver 1985*. (L.G. Schultz, H. van Olphen, and F.A. Mumpton, editors). Clay Minerals Society, Boulder, Colordao.

Prost, R., Dameme, A., Huard, E., Driard, J. and Leydecker, J.P. (1989) Infrared study of structural OH in kaolinite, dickite, nacrite, and poorly crystalline kaolinite at 5 to 600 K. *Clays and Clay Minerals*, **37**, 464–468.

Reynolds, R.C. and Bish, D.L. (2002) The effects of grinding on the structure of a low-defect kaolinite. *American Mineralogist*, **87**, 1626–1630.

Rouxhet, P.G., Samudacheata, N., Jacobs, H., and Anton, O. (1977) Attribution of the OH stretching bands of kaolinite. *Clay Minerals*, **12**, 171–178.

Sato, H., Ono, K., Johnston, C.T., and Yamagishi, A. (2004) First-principle study of polytype structures of 1:1 dioctahedral phyllosilicates. *American Mineralogist*, **89**, 1581–1585.

Shoval, S., Yariv, S., Michaelian, K.H., Boudeulle, M., and Panczer, G. (1999a) Hydroxyl-stretching bands 'A' and 'Z' in Raman and infrared spectra of kaolinites. *Clay Minerals*, **34**, 551–563.

Shoval, S., Yariv, S., Michaelian, K.H., Lapides, I., Boudeuille, M., and Panczer, G. (1999b) A fifth OH-stretching band in IR spectra of kaolinites. *Journal of Colloid and Interface Science*, **212**, 523–529.

Shoval, S., Yariv, S., Michaelian, K.H., Boudeulle, M., and Panczer, G. (2001) Hydroxyl-stretching bands in curve-fitted micro-Raman, photoacoustic and transmission infrared spectra of dickite from St. Claire, Pennsylvania. *Clays and Clay Minerals*, **49**, 347–354.

Wang, S.L. and Johnston, C.T. (2000) Assignment of the structural OH stretching bands of gibbsite. *American Mineralogist*, **85**, 739–744.

White, A.F., Blum, A.E., Schulz, M.S., Vivit, D.V., Stonestrom, D.A., Larsen, M., Murphy, S.F., and Eberl, D.D. (1998) Chemical weathering in a tropical watershed, Luquillo Mountains, Puerto Rico: I. Long-term versus short-term weathering fluxes. *Geochimica et Cosmochimica Acta*, **62**, 209–226.

Zheng, H. and Bailey, S.W. (1994) Refinement of the nacrite structure. *Clays and Clay Minerals*, **42**, 46–52.

Zotov, A., Mukhamet-Galeev, A., and Schott, J. (1998) An experimental study of kaolinite and dickite relative stability at 150-300 degrees C and the thermodynamic properties of dickite. *American Mineralogist*, **83**, 516–524.

(*Received 14 December 2007; revised 16 June 2008; Ms. 0107; A.E. B. Lanson*)